http://dx.doi.org/10.5012/bkcs.2011.32.11.4049

Anti-inflammatory and PPAR Subtypes Transactivational Activities of Phenolics and Lignans from the Stem Bark of *Kalopanax pictus*

Tran Hong Quang,[†,‡] Nguyen Thi Thanh Ngan,[†] Chau Van Minh,[‡] Phan Van Kiem,[‡] Nguyen Xuan Nhiem,[†,‡] Bui Huu Tai,[†] Nguyen Phuong Thao,[†,‡] Bui Thi Thuy Luyen,[†] Seok Bean Song,[†] and Young Ho Kim[†,*]

[†]*College of Pharmacy, Chungnam National University, Daejeon 305-764, Korea.* [*]*E-mail: yhk@cnu.ac.kr*
[‡]*Institute of Marine Biochemistry, Vietnam Academy of Science and Technology (VAST), 18 Hoang Quoc Viet, Caugiay, Hanoi, Viet Nam*
Received August 25, 2011, Accepted September 26, 2011

A new compound, kalopanaxin F (**3**), and 11 known compounds (**1**, **2**, **4-12**), were isolated from the stem bark of *Kalopanax pictus*. Their structures were elucidated on the basis of chemical and spectroscopic methods. Five of the compounds (**2**, **3**, **5**, **6**, and **12**) significantly inhibited TNFα-induced NF-κB transcriptional activity in HepG2 cells in a dose-dependent manner, with IC_{50} values ranging from 6.2 to 9.1 μM. Furthermore, the transcriptional inhibitory function of these compounds was confirmed based on decreases in COX-2 and iNOS gene expression in HepG2 cells. Compounds **3-7**, **9**, and **12** significantly activated the transcriptional activity of PPARs dose-dependently, with EC_{50} values ranging from 4.1-12.7 μM. Compounds **4** and **5** exhibited PPARα, PPARγ, and PPAR$\beta(\delta)$ transactivational activities in a dose-dependent manner, with EC_{50} values of 16.0 and 17.0, 8.7 and 16.5, 26.2 and 26.3 μM, respectively.

Key Words : *Kalopanax pictus*, Araliaceae, Phenolic, *Anti*-inflammatory, PPAR transactivational activity

Kalopanax pictus (Araliaceae) is a deciduous tree growing in East Asian countries. The stem bark of *K. pictus* has been used in traditional medicine to treat rheumatic arthritis, neurotic pain, and diabetes mellitus.[1] Phytochemical studies on the stem bark have demonstrated the presence of hederagenin glycosides, syringin, liriodendrin, and coniferylaldehyde glucosides,[2,3] and the methanol extract of the stem bark of *K. pictus* has been reported to possess cytotoxic,[4] antidiabetic,[5] and anti-inflammatory activities.[6] In this report, a new compound (**3**) and 11 known compounds (**1**, **2** and **4-12**) were isolated from the methanol extract of the stem bark of *K. pictus*.

Nuclear Factor-kappa B (NF-κB) is an inducible transcription factor of the Rel family, sequestered in the cytoplasm by the IκB family of proteins. NF-κB exists in several dimeric forms, but the p50/p65 heterodimer is the predominant one.[7] Activation of NF-κB by stimuli, including inflammatory cytokines such as TNF-α and IL-1, T-cell activation signals, growth factors, and stress inducers leads to phosphorylation and proteasome dependent degradation of IκB, leading to the release of free NF-κB.[7,8] This free NF-κB then binds to its target sites (κB sites in the DNA), to initiate transcription. This transcription has been known to be involved in a number of diseases including cancer, AIDS, and inflammatory disorders.[7,8] Hence inhibition of NF-κB signaling has become a therapeutic target for the treatment of inflammatory and cancer diseases. The effects of compounds **1-12** on TNFα (tumor necrosis factor α)-induced NF-κB transcriptional activity in HepG2 cells were evaluated. To confirm the inhibitory effects of the compounds on NF-κB transcriptional activity, we investigated the effects of the compounds on the upregulation of the pro-inflammatory proteins iNOS (inducible nitric oxide synthase) and COX-2 (cyclooxygenase-2) in TNFα-stimulated HepG2 cells.

The peroxisome proliferator-activated receptors (PPARs) form a subfamily of the nuclear receptor superfamily, of which three isoforms, PPARα, PPARγ, and PPAR $\beta(\delta)$ have been identified. PPARs regulate the expression of genes involved in the regulation of glucose, lipid, and cholesterol metabolism by binding to specific peroxisome proliferator response elements (PPREs) in the enhancer sites of regulated genes.[9-12] Accordingly, compounds that modulate the functions of PPARs are attractive for the treatment of type 2 diabetes, obesity, metabolic syndrome, inflammation, and cardiovascular disease.[13] Thus, we initially investigated the effects of compounds **1-12** on the transcriptional activity of PPARs in human hepatocarcinoma (HepG2) cells. Although the PPAR subtypes share a high level of sequence and structural homology, each has distinct physiological functions and each PPAR subtype exhibits a unique tissue expression pattern.[14] Thus, with the aim to understand how specifically the compounds modulate PPAR transcriptional activity, we further examined the transactivational effects of the compounds on the individual PPAR subtypes, PPARα, γ, and $\beta(\delta)$.

The known compounds were identified to be syringic acid-4-*O*-α-L-rhamnoside (**1**),[15] kalopanaxin B (**2**),[3] caffeic acid (**4**),[16] coniferin (**5**),[3] kalopanaxin A (**6**),[3] sinapic aldehyde 4-*O*-β-D-glucopyranoside (**7**),[17] pinoresinol (**8**),[18] (+)-pinoresinol *O*-β-D-glucopyranoside (**9**),[19] (+)-pinoresinol di-*O*-β-D-glucopyranoside (**10**),[19] (+)-syringaresinol *O*-β-D-glucopyranoside (**11**),[20] and liriodendrin (**12**),[19] by comparison of the NMR and MS data with those reported in the literature.

Table 1. ^{1}H (600 MHz) and ^{13}C NMR (150 MHz) Data for Compounds **2** and **3**

Position	**2**[a]		**3**[b]	
	δ_H	δ_C	δ_H	δ_C
1		132.7		130.3
2	7.06 (d, 2.4)	110.8	7.21 (d, 2.4)	112.4
3		150.4		151.0
4		147.4		150.4
5	7.45 (d, 7.2)	116.6	6.98 (d, 7.8)	117.1
6	6.93 (dd, 7.2, 2.4)	119.6	6.70 (dd, 7.8, 2.4)	124.0
7	6.81 (d, 16.2)	129.3	7.47 (d, 15.6)	155.0
8	6.52 (m)	130.3	6.60 (dd, 15.6, 7.8)	128.1
9	4.52 (d, 4.2)	63.1	9.59 (d, 7.8)	196.0
3-OCH_3	3.59 (s)	55.8	3.88 (s)	56.6
5-OCH_3				
1′		126.5		127.1
2′	7.45 (br s)	107.7	7.28 (br s)	107.6
3′		153.9		154.5
4′		139.8		140.0
5′		153.9		154.5
6′	7.45 (br s)	107.7	7.28 (br s)	107.6
7′		166.3		167.1
3′, 5′-OCH_3		56.1	3.84 (s)	56.6
1″	5.58 (d, 7.8)	102.4	4.98 (d, 7.8)	101.8
2″	4.29 (m)	75.7	3.51 (m)	74.7
3″	4.30 (m)	78.5	3.50 (m)	77.8
4″	4.13 (m)	71.7	4.12 (m)	72.0
5″	4.30 (m)	74.9	3.80 (m)	75.5
6″	5.28 (dd, 10.8, 1.8) 4.89 (m)	65.5	4.66 (dd, 11.4, 2.4) 4.48 (m)	65.2
1‴	6.09 (d, 1.2)	103.8	5.31 (d, 1.2)	103.4
2‴	4.88 (m)	72.2	4.22 (m)	71.2
3‴	4.74 (m)	72.7	4.21 (m)	71.3
4‴	4.30 (m)	73.8	3.40 (m)	73.6
5‴	4.13 (m)	71.7	3.91 (m)	72.0
6‴	1.61 (d, 6.6)	18.7	1.82 (d, 6.0)	17.9

[a]Spectra were recorded in C_5D_5N. [b]in CD_3OD. Coupling constants (J) are in Hz. Assignments were confirmed by HMQC and HMBC spectra.

Compound **3** was isolated as a white amorphous powder, and its molecular formula was established to be $C_{31}H_{38}O_{16}$ by HR-ESI-TOF MS at *m/z* 665.2092 $[M-H]^-$ (calcd for $C_{31}H_{37}O_{16}$, 665.2082). The IR spectrum of **3** revealed hydroxyl, carboxyl, and aldehyde groups based on absorption bands at 3396, 1714, and 1666 cm^{-1}, respectively. The ^{1}H NMR spectrum revealed the presence of an aromatic ring with ABX spin system [δ_H 7.21 (1H, d, J = 2.4 Hz, H-2), 6.98 (1H, d, J = 7.8 Hz, H-5), and 6.70 (1H, dd, J = 7.8, 2.4 Hz, H-6)], an aromatic ring with AX spin system [δ_H 7.28 (2H, br s, H-2' and H-6')], an olefin [δ_H 7.47 (1H, d, J = 15.6 Hz, H-7) and 6.60 (1H, dd, J = 15.6, 7.8 Hz, H-8)], an aldehyde group at δ_H 9.59 (1H, d, J = 7.8 Hz, H-9), and three methoxyl groups at δ_H 3.88 (3H, s) and 3.84 (6H, s) (Tables 1). In addition, two anomeric protons were also observed at δ_H 4.98 (1H, d, J = 7.8 Hz), and 5.31 (1H, d, J = 1.2 Hz) in the ^{1}H NMR spectrum, indicating that **3** possessed two sugar

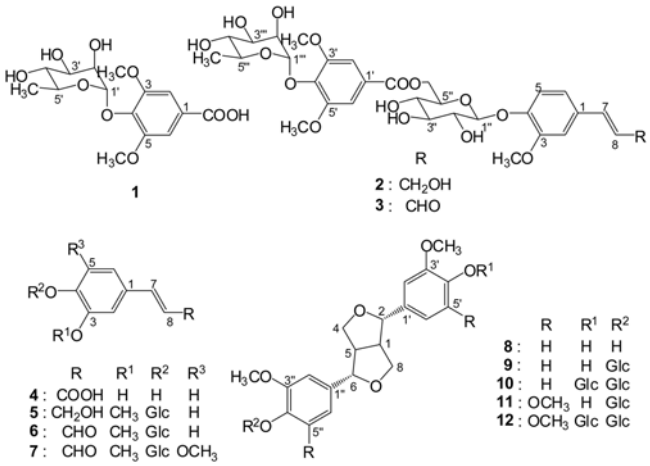

Figure 1. Structures of compounds **1-12**.

units. By acid hydrolysis and GC alnalysis, the sugar units were identified as D-glucose and L-rhamnose. The α-configuration of the rhamnopyranosyl moiety was determined from the small coupling constant (J = 1.2 Hz) and the β-configuration of the glucopyranosyl moiety was identified from the relative large coupling constant (J = 7.8 Hz) for the anomeric protons in the ^{1}H NMR spectrum (Table 1). The ^{13}C NMR and DEPT spectra exhibited 31 carbon signals, including four methyl, one methylene, 18 methine, and eight quaternary carbons. The ^{13}C NMR of **3** showed the presence of an aldehyde group (δ_C 196.0, C-9), a carboxyl group (δ_C 167.1, C-7'), and two anomeric carbons [δ_C 101.7 (C-1") and 103.4 (C-1‴)] (Tables 1). The HMBC correlations of H-1 of the glucose (δ_H 4.98) with C-4 (δ_C 150.4), and H-1 of the rhamnose (δ_H 5.31) with C-4' (δ_C 140.0) suggested that the glucose and rhamnose attached to C-4 and C-4' of the aglycone of **3**, respectively (Figure 2). Comparison of the NMR data of compound **3** with those of **2** revealed that the structures of these compounds were similar to each other (Table 1), except for the conversion of an oxymethylene (C-9) in **2** to an aldehyde group (δ_C 196.0, C-9) in **3**. Based on the data obtained, the structure of **3** was established as coniferin aldehyde 6'-*O*-(4-*O*-α-L-rhamnopyranosyl)-syringate, named kalopanaxin F.

The *anti*-inflammatory activity of compounds **1-12** was evaluated through inhibition of a TNFα-induced NF-κB luciferase reporter and by attenuation of TNFα-induced pro-inflammatory gene (iNOS and COX-2) expression in HepG2 cells (see Experimental). The results showed that compounds **2**, **3**, **5**, **6**, and **12** significantly inhibited TNFα-induced

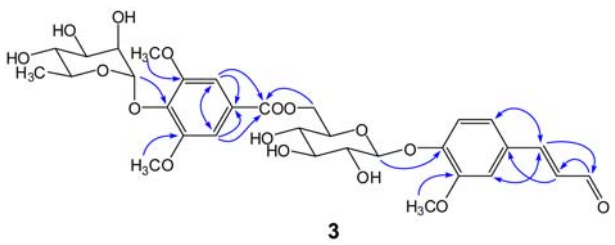

Figure 2. Key HMBC correlations of compound **3**.

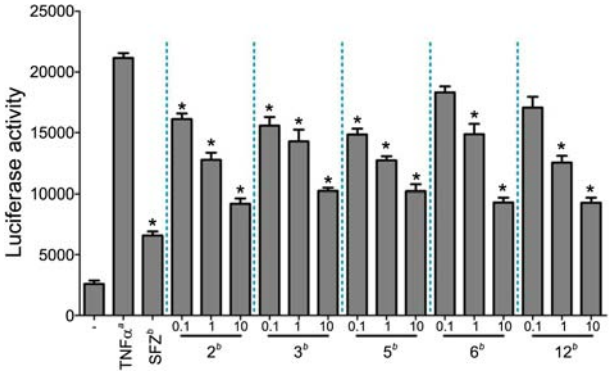

Figure 3. Effects of compounds **2**, **3**, **5**, **6**, and **12** on the TNFα-induced NF-κB luciferase reporter activity in HepG2 cells. The values are mean ± SD (n = 3). [a]Stimulated with TNFα. [b]Stimulated with TNFα in the presence of **2**, **3**, **5**, **6**, and **12** (0.1, 1, and 10 μM), and sulfasalazine. SFZ: sulfasalazine, positive control (10 μM). Statistical significance is indicated as * (p <0.05) as determined by Dunnett's multiple comparison test.

NF-κB transcriptional activity in HepG2 cells in a dose-dependent manner (Figure 3), with IC_{50} values ranging from 6.2 to 9.1 mM (Table 2). Compounds **1**, **4**, and **7-11** showed no activity at tested concentrations.

Since NF-κB is an important transcription factor involved in regulating the expression of inflammatory NF-κB target genes such as iNOS and COX-2,[21,22] we investigated the effects of compounds **2**, **3**, **5**, **6**, and **12** on the expression of these genes in TNFα-stimulated HepG2 cells using RT-PCR (see Experimental). Consistent with their inhibitory activity toward NF-κB, compounds **2**, **3**, **5**, **6**, and **12** significantly inhibited the induction of COX-2 and iNOS mRNA in a dose-dependent manner (Figure 4), indicating that these compounds attenuated transcription of these genes. Moreover, the housekeeping protein b-actin was not changed by the presence of compounds **2**, **3**, **5**, **6**, and **12** at the same concentration.

Table 2. Inhibitory Effects of Compounds **1-12** on the TNFα-induced NF-κB transcriptional activity

Compound	IC_{50} (μM)
2	6.2 ± 0.6
3	9.1 ± 0.5
5	8.6 ± 1.2
6	7.9 ± 0.6
12	6.5 ± 0.8
Sulfasalazine	0.9 ± 0.2

The values are mean ± SD (n = 3). Compounds **1**, **4**, and **7-11** were in active at tested concentrations.

The effects of compounds **1-12** on the activation of PPARs were evaluated using a PPRE luciferase reporter assay (see Experimental). The results showed that compounds **3-7**, **9** and **12** significantly activated the transcriptional activity of PPARs in a dose-dependent manner (Figure 5), with EC_{50} values ranging from 4.1-12.7 μM, whereas compounds **1**, **2**,

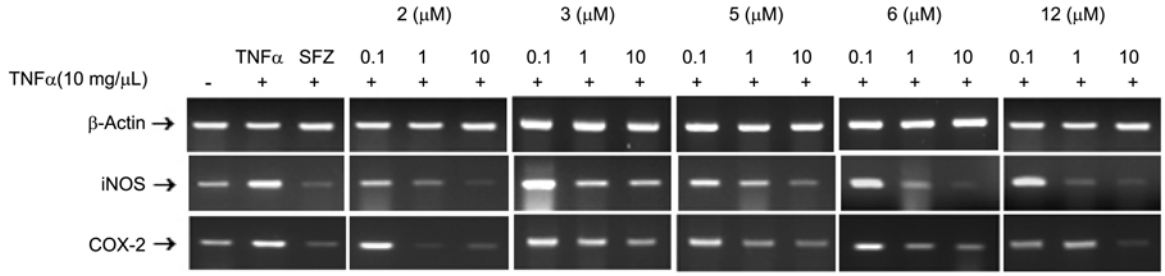

Figure 4. Effects of compounds **2**, **3**, **5**, **6**, and **12** on iNOS and COX-2 mRNA expression in HepG2 cells.

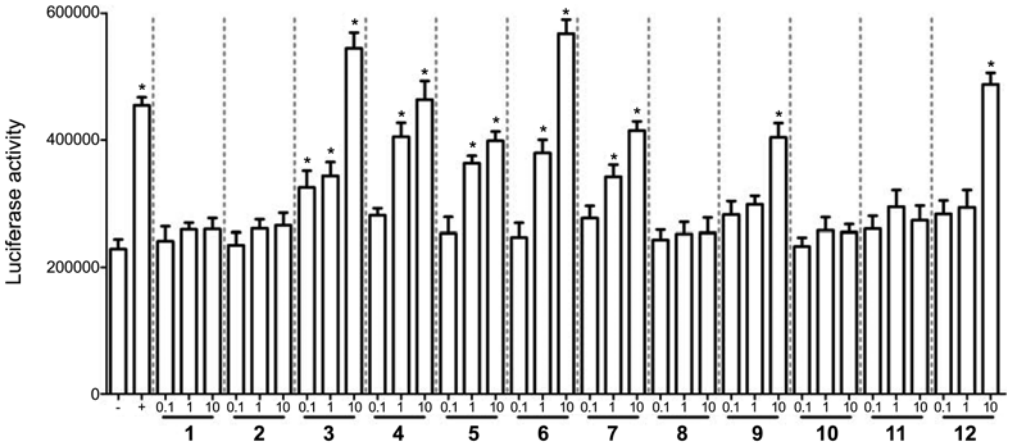

Figure 5. PPARs transactivational activity of compounds **1-12** in HepG2 cells. (–): vehicle group. (+): positive control (1 μM): benzafibrate. *Significantly different from vehicle group (P < 0.05).

Table 3. PPAR transactivational activities of compounds **1-12**

Compound	EC_{50} (μM)			
	PPARs	Gal4/ PPARα-LBD	Gal4/ PPARγ-LBD	Gal4/ PPAR$\beta(\delta)$-LBD
1	> 40*	> 40	> 40	> 40
2	> 40	> 40	> 40	> 40
3	4.1 ± 0.1	> 40	> 40	> 40
4	6.6 ± 0.6	16.0 ± 1.0	8.7 ± 0.8	26.2 ± 1.8
5	12.7 ± 0.6	17.0 ± 0.2	16.5 ± 1.2	26.3 ± 1.2
6	3.0 ± 0.5	39.7 ± 1.3	> 40	> 40
7	12.1 ± 0.7	> 40	31.3 ± 2.1	> 40
8	> 40	> 40	> 40	> 40
9	12.5 ± 0.9	> 40	26.2 ± 1.7	> 40
10	> 40	> 40	> 40	> 40
11	> 40	> 40	> 40	> 40
12	8.1 ± 0.1	20.6 ± 1.3	> 40	> 40
Benzafibrate	1.14 ± 0.07			
Ciprofibrate		0.80 ± 0.02		
Troglitazone			0.64 ± 0.04	
L-165.041				0.54 ± 0.05

EC_{50}: the concentration of test compound that gave 50% of the maximal reporter activity. *A compound is considered inactive with EC_{50} > 40 μM.

8, **10** and **11** were not active at the tested concentrations (Table 3). From these primary data, with the aim of understanding how specifically the compounds **3-7**, **9**, and **12** modulate PPAR transcriptional activity, we further examined the PPAR transactivational effects of the compounds on individual PPAR subtypes, including PPARα, γ, and $\beta(\delta)$ (Figures 6-8).

Among the compounds tested, compounds **4**, **5**, and **12** exhibited PPARα transactivational activity in a dose-dependent manner, with EC_{50} values of 16.0, 17.0, and 20.6 μM, respectively (Table 3). Compounds **4**, **5**, **7**, and **9** activated the transcriptional activity of PPAR γ with EC_{50} values of 8.7, 16.5, 31.3, and 26.2 μM, whereas compounds **4** and **5** showed PPAR $\beta(\delta)$ transactivational activity with EC_{50} values of 26.2 and 26.3 μM (Table 3).

Cell viability, as measured by the MTT [3-(4,5-dimethylthiazole-2-yl)-2,5-diphenyltetrazolium bromide] colorimetric method,[23] showed that compounds **1-12** had no significant cytotoxicity in HepG2 cells at tested concentrations (data not shown).

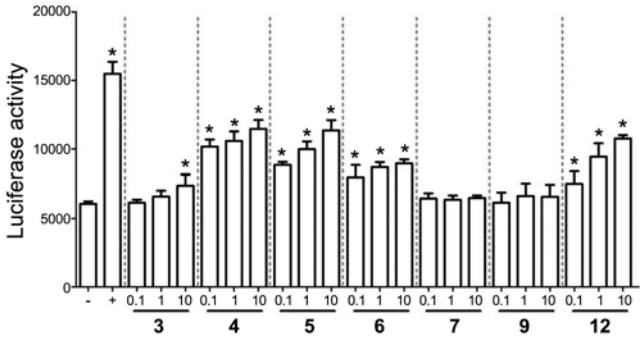

Figure 6. PPARα transactivational activity of compounds **3-7**, **9**, and **12** in HepG2 cells. (–): vehicle group. (+): positive control (1 μM): ciprofibrate. *Significantly different from vehicle group (P < 0.05).

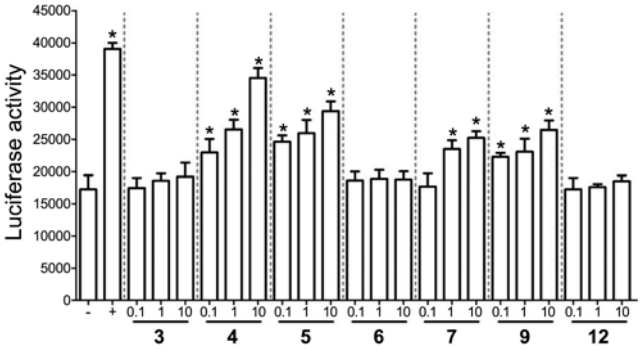

Figure 7. PPARγ transactivational activity of compounds **3-7**, **9**, and **12** in HepG2 cells. (–): vehicle group. (+): positive control (1 μM): troglitazone. *Significantly different from vehicle group (P < 0.05).

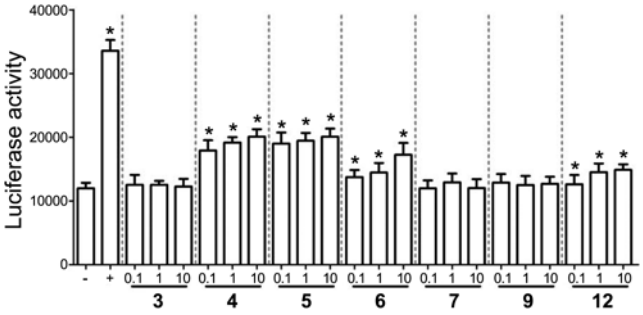

Figure 8. PPAR$\beta(\delta)$ transactivational activity of compounds **3-7**, **9**, and **12** in HepG2 cells. (–): vehicle group. (+): positive control (1 μM): L-165.041. *Significantly different from vehicle group (P < 0.05).

Experimental

General Procedures. Optical rotation was determined using a Jasco DIP-370 digital polarimeter. The FT-IR spectra were measured using a Jasco Report-100 infrared spectrometer. Electrospray ionization (ESI) mass spectra were obtained using an Agilent 1200 LC-MSD Trap spectrometer. Gas chromatography was carried out on a Shidmazu-2010 spectrometer, detector: FID, detection temperature: 300 °C, column: SPB-1 (0.25 mm i.d. × 30 m), column temperature: 230 °C, carrier gas He (2 mL/min), injection temperature: 250 °C, injection volume: 0.5 μL. HR-ESI-TOF mass spectra were obtained using a JEOL JMS-T100LC spectrometer. The NMR spectra were recorded on a Jeol ECA 600 spectrometer using TMS as an internal standard. TLC was performed on Kieselgel 60 F254 (1.05715; Merck, Darmstadt, Germany) or RP-18 F254s (Merck) plates. Spots were visualized by spraying with 10% aqueous H_2SO_4 solution, followed by heating. Column chromatography (CC) was performed on silica gel (Kieselgel 60, 70-230 mesh and 230-400 mesh, Merck) and YMC RP-18 resins.

Plant Materials. The stem bark of of *K. pictus* was purchased from herbal market at Kumsan, Chungnam, Korea, in August 2009. The plant material was identified by one of us (Y. H. Kim). A voucher specimen (CNU09105) was deposited at herbarium, College of Pharmacy, Chungnam National University.

Extraction and Isolation. The dried stem bark of *K. pictus* (3 kg) was extracted with hot MeOH. After concentration, the MeOH extract (290 g) was suspended in water and then partitioned successively with *n*-hexane, CH_2Cl_2, and EtOAc to give *n*-hexane (A), CH_2Cl_2 (B), EtOAc (C) and water (D) fractions, respectively. Fraction D was chromatographed on a column of highly porous polymer (Diaion HP-20) and eluted with H_2O and MeOH, successively to give three fractions (D1-D3). Fraction D1 was then separated by column chromatography over silica gel, using CH_2Cl_2-MeOH-H_2O (5:1:0.1) as eluents, and further purified by YMC reverse-phase chromatography, eluting with MeOH-H_2O (2:1) to afford **4** (55 mg) and **5** (60 mg). Fraction D2 was chromatographed over silica gel, eluting with MeOH in CH_2Cl_2 (0-100%, step-wise) to provide five subfractions (D2A-D2E). Subfraction D2B was separated by YMC reverse-phase chromatography, using MeOH-H_2O (1:1) as eluent to give two subfractions (D2B1 and D2B2). Subfraction D2B1 was then chromatographed over silica gel column, using CH_2Cl_2-MeOH (5:1) to obtain **6** (5 mg) and **7** (5 mg). Subfraction D2B2 was further purified by column chromatography over silica gel, eluting with EtOAc-MeOH-H_2O (15:1:0.1) to obtain **8** (7 mg), **9** (15 mg), and **11** (12 mg). Subfraction D2C was separated by YMC reverse-phase chromatography, using MeOH-H_2O (15:10) as eluent, and further purified by column chromatography over silica gel, eluting with CH_2Cl_2-MeOH- H_2O (5:1:0.1) to obtain **1** (4 mg) and **2** (20 mg) and **3** (8 mg). Subfraction D2D was separated by YMC reverse-phase chromatography, eluting with MeOH-H_2O (1:1), and further purified by column chromatography over silica gel, using CH_2Cl_2-MeOH-H_2O (4:1:0.1) as eluents to give **10** (15 mg) and **12** (57 mg).

Kalopanaxin B (2): white, amorphous powder; $[\alpha]_D^{25}$ −74.9 (*c* 0.5, MeOH); FT-IR (CH_3CN) ν_{max} 3329, 2932, 1707, 1584, 1449, 1410, 1227, 1120, 1072, 968 cm^{-1}. ^1H NMR (C_5D_5N, 600 MHz) and ^{13}C NMR data (C_5D_5N, 150 MHz), see Table 1; ESI-MS *m/z* 669 $[M + H]^+$.

Kalopanaxin F (3): white, amorphous powder; $[\alpha]_D^{25}$ −47.7 (*c* 0.04, MeOH); FT-IR (CH_3CN) ν_{max} 3396, 2935, 1714, 1666, 1594, 1509, 1462, 1416, 1335, 1272, 1219, 1128, 1067, 965 cm^{-1}. ^1H NMR (CD_3OD, 600 MHz) and ^{13}C NMR data (CD_3OD, 150 MHz), see Table 1; HR-ESI-TOF MS *m/z* 665.2092 $[M-H]^-$ (calcd for $C_{31}H_{37}O_{16}$, 665.2082).

Acid Hydrolysis and Sugar Identification. Compound **3** (3 mg) was heated in 3 mL of 10% HCl-dioxane (1:1) at 80 °C for 3 h. After the solvent was removed *in vacuo*, and the residue was partitioned between EtOAc and H_2O to give the aglycone and the sugar, respectively. The sugar components in the aqueous layer were analyzed by silica gel TLC by comparison with standard sugars. The solvent system was CH_2Cl_2-MeOH-H_2O (2:1:0.2), and spots were visualized by spraying with 95% EtOH-H_2SO_4-anisaldehyde (9:0.5:0.5, v/v), then heated at 180 °C for 5 min. For sugars, the R_f of glucose and rhamnose by TLC was 0.30 and 0.75, respectively. The results were confirmed by GC analysis as follows. The aqueous layer was evaporated to dryness to give a residue, and was dissolved in anhydrous pyridine (100 mL) and then mixed with a pyridine solution of 0.1 M L-cysteine methyl ester hydrochloride (100 μL). After warming at 60 °C for 2 h, trimethylsilylimidazole solution were added and warmed at 60 °C for 2 h. The mixture was then evaporated *in vacuo* to give a dried product, which was partitioned between *n*-hexane and H_2O. The *n*-hexane layer was filtered and analyzed by GC. The retention times of the persilylated monosaccharide derivatives were as follows: L-rhamnose (t_R, 5.31 min) and D-glucose (t_R, 14.11 min), were confirmed by comparison with those of authentic standards.

***In Vitro* Anti-inflammatory Assay.**

NF-κB-luciferase Assay: The NF-κB-Luciferase plasmid was first transfected into HepG2 cells. After a limited amount of time, the cells were lysed and luciferin, the substrate of luciferase, was introduced into the cellular extract along with Mg^{2+} and an excess of ATP. Under these conditions, luciferase enzymes expressed by the reporter vector could catalyze the oxidative carboxylation of luciferin. Cells were seeded at 1.5×10^5 cells per well in 12-well plates and grown for 24 h. All cells were transfected using WelFect M^{TM} Gold (WelGENE Inc, Daegu, South Korea), as guided by the manufacturer. Luciferase activity was assayed using an LB 953 Autolumat (EG&G Berthold, Nashua, NH).[24] The transfected HepG2 cells were pretreated for 1 h with either vehicle (DMSO) and compounds, followed by 1 h of treatment with 10 ng/mL TNFα. Unstimulated HepG2 cells were used as a vehicle group (−). Cells were then harvested, and luciferase activity was assayed. The NF-κB-Luciferase plasmid was kindly provided by Dr. Kyoon E. Kim (Chungnam National University, Daejeon, Korea).

RNA Preparation and Reverse Transcriptase Polymerase Chain Reaction (RT-PCR): Total RNA was extracted using Easy-blue reagent (Intron Biotechnology, Seoul, Korea). Approximately 2 μg total RNA was subjected to reverse transcription using Moloney murine leukemia virus (MMLV) reverse transcriptase and oligo-dT primers (Promega, Madison, WI) for 1 h at 42 °C. PCR for synthetic cDNA was performed using a Taq polymerase pre-mixture (TaKaRa, Japan). The PCR products were separated by electrophoresis on 1% agarose gels and stained with EtBr. PCR was conducted with the following primer pairs: iNOS sense 5'-TCATCCGCTATGCTGGCTAC-3', iNOS antisense 5'-CTCAGGGTCACGGCCATTG-3', COX-2 sense 5'-GCCCAGCACTTCACGCATCAG-3', COX-2 antisense 5'-GACCAGGCACCAGACCAAAGACC-3', β-actin sense 5'-TCACCCACACTGTGCCCATCTACG-3', and β-actin antisense 5'-CAGCGGAACCGCTCATTGCCAATG-3'. The specificity of products generated by each set of primers was examined using gel electrophoresis and further confirmed by a melting curve analysis.

HepG2 cells were pretreated in the absence and presence of compounds for 1 h, then exposed to 10 ng/mL TNFα for 6 h. Total mRNA was prepared from the cell pellets using Easy-blue. The levels of mRNA were assessed by RT-PCR.

PPAR Transactivational Assay.

Cell Culture and Reagents: Human hepatocarcinoma HepG2 cells were maintained in DMEM (Invitrogen, Carlsbad, CA) containing 10% heat-inactivated fetal bovine serum (FBS), 100 units/mL penicillin, 10 μg/mL streptomycin at 37 ^{o}C and 5% CO_2.

PPRE-luciferase Assay: Human hepatoma cells (HepG2) were seeded at 1.5×10^5 cells per well in 12-well plates and grown for 24 h before transfection. An optimized amount of DNA plasmid (0.5 μg PPRE-Luc and 0.2 μg PPAR-inpCMV) was diluted in 100 μL Dulbecco's modified Eagle medium (DMEM). All cells were transfected with the plasmid mixture using WelFect M^{TM} Gold (WelGENE Inc, Daegu, South Korea) as described by the manufacturer. After 30 min of incubation at room temperature, the DNA plasmid solution (100 μL) was introduced and mixed gently with cells. After 24 h of transfection, the medium was changed to TOM^{TM} (Transfection Optimized Medium, Invitrogen, Carlsbad, CA) containing 0.1 mM NEAA, 0.5% charcoal- stripped FBS, and the individual compounds (test group), dimethyl sulfoxide (vehicle group), or benzafibrate (positive control group). The cells were then cultured for 20 h. Next, the cells were washed with PBS and harvested with 1× passive lysis buffer (200 μL). The intensity of emitted luminescence was determined using an LB 953 Autolumat (EG&G Berthold, Bad Wildbad, Germany). The PPRE-Luc plasmid was provided by Dr. Kyoon E. Kim (Chungnam National University, Daejeon, Korea).

PPAR Subtype Specific Transactivational Assay. Human hepatoma cells (HepG2) were seeded at 1.5×10^5 cells per well in 12-well plates and grown for 24 h before transfection. Cells were transfected separately with one pGal4-PPAR subfamily vector [pFA-Gal4-PPARα-LBD, pFA-Gal4-PPARγ-LBD, or pFA-Gal4-PPAR$\beta(\delta)$-LBD expression plasmids, provided by Dr. Young Yang, Sookmyung Women's University, Seoul, Korea] together with pFR-Luc using the WelFect M^{TM} Gold transfection reagent (WelGENE Inc, Daegu, South Korea), as described by the manufacturer. After 24 h of transfection, the medium was changed to TOM^{TM} (Transfection Optimized Medium, Invitrogen, Carlsbad, CA) containing 0.1 mM NEAA, 0.5% charcoal-stripped FBS, and each compound (test group), dimethyl sulfoxide (vehicle group), ciprofibrate (positive control group for PPARα), troglitazone (positive control group for PPARγ) or L-165.041 [positive control group for PPAR$\beta(\delta)$]. The cells were then cultured for 20 h. After which the cells were washed with PBS and harvested with 1× passive lysis buffer (200 μL). The intensity of emitted luminescence was determined using a Centro LB 960 microplate luminometer (EG&G Berthold, Bad Wildbad, Germany) by measuring light emission for 5 s.

Statistical Analysis. All data represent the mean ± SD of at least three independent experiments performed in triplicates. Statistical significance is indicated as * (p <0.05) as determined by one-way ANOVA followed by Dunnett's multiple comparison test.

Acknowledgments. This work was supported by a grant from the Korea Food and Drug Administration for Studies on Standardization of Herbal Medicine (2010) and Priority Research Center Program through the National Research Foundation of Korea (NRF) funded by the Ministry of Education, Science and Technology (2009-0093815), Republic of Korea.

References

1. Kim, T. J. Seoul National University Press: Seoul, 1996; Vol. 2, pp 169.
2. Shao, C. J.; Kasai, R.; Xu, J. D.; Tanaka, O. *Chem. Pharm. Bull.* **1989**, *37*, 311.
3. Sano, K.; Sanada, S.; Ida, Y.; Shoji, J. *Chem. Pharm. Bull.* **1991**, *39*, 865.
4. Lee, K.-T.; Sohn, I.-C.; Park, H.-J.; Kim, D.-W.; Jung, G.-O.; Park, K.-Y. *Planta Med.* **2000**, *66*, 329.
5. Park, H.-J.; Kim, D.-H.; Choi, J.-W.; Park, J.-H.; Han, Y.-N. *Arch. Pharm. Res.* **1998**, *21*, 24.
6. Lee, E. B.; Li, D. W.; Hyun, J. E.; Kim, I. H.; Whang, W. K. *J. Ethnopharmacol.* **2001**, *77*, 197.
7. Pande, V.; Ramos, M. J. *Curr. Med. Chem.* **2005**, *12*, 357.
8. Baldwin, A. S., Jr. *J. Clin. Invest.* **2001**, *107*, 3.
9. Berger, J.; Moller, D. E. *Annu. Rev. Med.* **2002**, *53*, 409.
10. Balint, B. L.; Nagy, L. *Endocr. Metab. Immune Disord. Drug Targets* **2006**, *6*, 33.
11. Barish, G. D.; Narkar, V. A.; Evans, R. M. *J. Clin. Invest.* **2006**, *116*, 590.
12. Haluzik, M. M.; Haluzik, M. *Physiol. Res.* **2006**, *55*, 115.
13. Kuroda, M.; Mimaki, Y.; Honda, S.; Tanaka, H.; Yokota, S.; Mae, T. *Bioorg. Med. Chem.* **2010**, *18*, 962.
14. Shearer, B. G.; Billin, A. N. *BBA-Mol. Cell. Biol. L.* **2007**, *1771*, 1082.
15. Wang, Y. L.; Li, Y. J.; Wang, A. M.; He, X.; Liao, S. G.; Lan, Y. Y. *J. Asian Nat. Prod. Res.* **2010**, *12*, 765.
16. Maggi-Capeyron, M. F.; Ceballos, P.; Cristol, J. P.; Delbosc, S.; Le Doucen, C.; Pons, M.; Leger, C. L.; Descomps, B. *J. Agric. Food. Chem.* **2001**, *49*, 5646.
17. Ida, I.; Satoh, Y.; Ohtsuka, M.; Nagasao, M.; Shoji, J. *Phytochemistry* **1994**, *35*, 209.
18. Vermes, B.; Seligmann, O.; Wagner, H. *Phytochemistry* **1991**, *30*, 3087.
19. Deyama, T. *Chem. Pharm. Bull.* **1983**, *31*, 2993.
20. Kobayashi, H.; Karasawa, H.; Miyase, T.; Fukushima, S. *Chem. Pharm. Bull.* **1985**, *33*, 1452.
21. Wong, H. R.; Menendez, I. Y. *Biochem. Biophys. Res. Commun.* **1999**, *262*, 375.
22. Pahl, H. L. *Oncogene* **1999**, *18*, 6853.
23. Scudiero, D. A.; Shoemaker, R. H.; Paull, K. D.; Monks, A.; Tierney, S.; Nofziger, T. H.; Currens, M. J.; Seniff, D.; Boyd, M. R. *Cancer Res.* **1988**, *48*, 4827.
24. Kim, K. K.; Park, K. S.; Song, S. B.; Kim, K. E. *Mol. Carcinog.* **2010**, *49*, 259.